

## Phonon Softening and Elastic Instabilities in the Cubic-to-Orthorhombic Structural Transition of CsH

A. M. Saitta,<sup>1,\*</sup> D. Alfè,<sup>1,\*</sup> S. de Gironcoli,<sup>1,\*</sup> and S. Baroni,<sup>1,2,\*</sup>

<sup>1</sup>*INFN—Istituto Nazionale per la Fisica della Materia and SISSA—Scuola Internazionale Superiore di Studi Avanzati, Via Beirut 2-4, I-34014 Trieste, Italy*

<sup>2</sup>*CECAM—Centre Européen de Calcul Atomique et Moléculaire, ENSL, 46 Allée d'Italie, 69364 Lyon Cedex 07, France*  
(Received 21 October 1996)

The cubic-to-orthorhombic structural transition occurring in CsH at a pressure of about 17 GPa is studied by *ab initio* calculations. The relative stability of the competing structures and the transition pressure are correctly predicted. We show that this pressure-induced first-order transition is intimately related to a displacive second-order transition which would occur upon application of a shear strain to the (110) planes. The resulting instability is rationalized in terms of the pressure-induced modifications of the electronic structure. [S0031-9007(97)03462-5]

PACS numbers: 64.70.Kb, 62.50.+p, 63.20.Dj, 63.70.+h

In recent years the availability of the diamond anvil-cell technology [1] has renewed the interest in the high-pressure properties of alkali halides which are the simplest and prototypical among ionic solids. In the case of cesium halides, these studies have been carried out especially in the search of band-overlap metallization which occurs at pressures in the Mbar range. In the quest of metallization, unexpected phase transformations to tetragonal and orthorhombic structures have been observed experimentally [2–6] and studied theoretically [6–9].

Metal hydrides are considerably more covalent than the corresponding halides. In fact, transition-metal hydrides are considered to be covalent materials, whereas alkali hydrides are structurally rather similar to the corresponding halides. Alkali hydrides at zero pressure crystallize in the rocksalt (cubic  $B1$ ) structure, while most of them undergo a transition to the cubic  $B2$  (CsCl-like) structure at an applied pressure of a few GPa [10–12]. Recently, a second transition from the  $B2$  structure to a new orthorhombic phase has been observed to occur in CsH at an applied pressure of about 17 GPa [13]. The new phase has been assigned the CrB structure which belongs to the  $D_{2h}^{17}$  space group.

In order to assess the driving mechanisms of this transition we have undertaken a series of first-principles calculations of the electronic, structural, elastic, and vibrational properties of CsH as well as of their dependence upon pressure. To this end, we have employed density-functional theory (DFT) within the local-density approximation (LDA) [14], and its gradient-corrected (GC) generalizations [15]. Our calculations have been performed using norm-conserving pseudopotentials [16]. In the case of Cs,  $5s$  and  $5p$  semicore states have been treated as valence states. For LDA calculations we have used the same Cs potential as in Ref. [8], while hydrogen is described by a norm-conserving pseudopotential constructed for the  $1s$  wave function, so as to smoothen it somewhat and make our calculations well converged with the 25 Ry kinetic-energy cutoff which we use. New potentials have been generated for GC calculations. The

vibrational properties are determined using the density-functional perturbation theory (DFPT) [17].

In Table I we report our results for some structural properties of CsH in the three phases studied here:  $B1$ ,  $B2$ , and CrB. The LDA fails to account for the stability of the rocksalt structure at zero pressure (negative  $B1 \rightarrow B2$  transition pressure), while GC calculations predict the correct sequence of transitions. GC-DFT also considerably improves the agreement between calculated and observed equilibrium lattice parameters and bulk moduli. The inclusion of Cs semicore states in the valence manifold implies that the pseudopotential transferability is optimal around the corresponding orbital energies, rather than at the energies of the valence states. As a consequence, this treatment of semicore states—although essential to obtain sensible results [8]—might require the use of more than one reference state in order to ensure optimum transferability. Whether or not the relatively poor quality of the LDA predictions is due to deficiencies in the Cs pseudopotential and the improvements achieved by using GC-DFT due to a fortuitous cancellation of errors is a matter which deserves further investigations. In any events, our results seem to confirm the importance of the gradient corrections to the LDA in the description of structural

TABLE I. Comparison between calculated and experimentally observed structural properties of CsH.  $a_0$  (a.u.) is the equilibrium lattice parameter in the  $B1$  phase,  $B_0$  (GPa) the bulk modulus,  $P_1^*$  and  $P_2^*$  the transition pressures (GPa) to the  $B2$  and CrB structures, respectively, while  $\Delta V_1$  and  $\Delta V_2$  are the corresponding volume changes.  $V_2^*/V_0$  is the ratio of the volume at the  $B2 \rightarrow$  CrB transition to the equilibrium volume.

	$a_0$	$B_0$	$P_1^*$	$\Delta V_1$	$P_2^*$	$\Delta V_2$	$V_2^*/V_0$
LDA	11.62	11.3	-0.8	18.0%	11	4.5%	0.63
GC	12.25	10.3	1.5	12.5%	15	4.0%	0.54
Expt. <sup>a</sup>	12.07	8.0	0.8	8.4%	17	6.3%	0.53

<sup>a</sup>Ref. [13].

phase transitions, recently claimed in the case of the diamond to  $\beta$ -tin transition in silicon [18]. Both LDA and GC-DFT calculations correctly predict that a transition from the  $B2$  to the CrB phases would occur at pressures somewhat larger than 10 GPa. In this case too, GC-DFT gives a value of the transition pressure in closer agreement with experiments (15 vs 17 GPa). Note, however, that—due to hysteresis effects—the experimental estimate done when loading the sample [13] only provides an upper limit to the transition pressure. Also the volume discontinuity and the ratio between the transition volume and the equilibrium one are well reproduced by our calculations.

In Ref. [13] it was noted that the CrB structure can be derived from the CsCl parent structure through a *displacive transition involving  $X_5^+$  or  $X_5^-$  mode softening*. We do not find any evidence of such a softening. The CrB structure can also be viewed as resulting from a continuous deformation of the cubic  $B2$  structure in which a shear of the cubic edges in the (110) planes is coupled to a microscopic distortion of the atomic lattice, having the periodicity of a zone-border transverse phonon at the  $M$  point of the Brillouin zone (BZ),  $\mathbf{q} = (\frac{1}{2}, \frac{1}{2}, 0)$ , with symmetry  $M_2^-$ , and polarized along (001). In Fig. 1 we display how the distorted (110) plane (lower panel) results from the combination of the shear (upper left) and the atomic (upper right) deformations. In the ideal CrB structure the  $a$  and  $b$  crystallographic parameters indicated in Fig. 1 are in the ratio  $b/a = 2\sqrt{2}$  which would be appropriate to a cubic structure. Because of

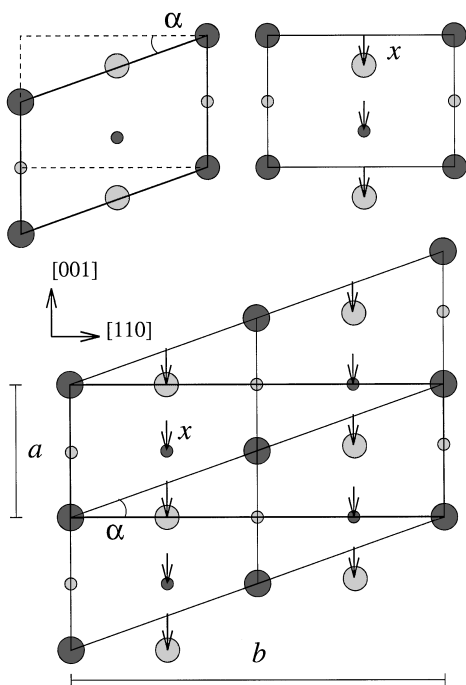


FIG. 1. Decomposition of the distortion leading to the CrB structure (lower panel) into a shear (upper left) and an atomic (upper right) contribution. Large and small circles represent Cs and H atoms, respectively. Dark and light shading refer to the topmost and second (110) layers, respectively.

the lower symmetry of the CrB structure with respect to the cubic one, the actual value of  $b/a$  slightly differs from the ideal one and depends somewhat on pressure. This dependence is, however, very weak: at the transition pressure, for instance, one has  $b/a \approx 2.9$ . The third crystallographic axis is orthogonal to the  $ab$  plane, and the corresponding crystallographic parameter has an ideal value  $c = \sqrt{2}a$ . The pressure dependence of  $c/a$  is somewhat stronger than that of  $b/a$ : at the transition, for instance, one has  $c/a \approx 1.3$ .

In order to understand the interplay between the shear and the atomic distortions in determining the pressure-induced structural instability of the CsCl phase and to disentangle their effects as much as possible, we have studied the energy landscape of our system as a function of the volume,  $V$ , and of the amplitudes of the shear and atomic deformations which we measure through the parameters  $t = \tan(\alpha) \times b/a$  and  $u = x/a$ , respectively [19]. At any given pressure, the stable phase is that which minimizes the enthalpy,  $H = E + PV$ . In Fig. 2 we show the enthalpy of the system as a function of amplitude of the shear deformation, as calculated by minimizing the energy with respect to  $u$ , at given values of  $V$  and  $t$ . We see that at any positive pressure a second minimum exists for  $t = 1$ , corresponding to the CrB orthorhombic structure. Actually, the exact value of  $\alpha$  slightly depends on pressure because so does  $b/a$ . For pressures higher than  $P_2^* \approx 11$  GPa the second minimum becomes more stable giving rise to a first-order phase transition. The amplitude of the atomic distortion which minimizes the enthalpy,  $u_{\min}$ , depends on  $t$ , but for  $t = 1$  (i.e., in the CrB phase) it is constrained by symmetry to be  $u_{\min} = 1/4$ , independent of pressure. The dependence of  $u_{\min}$  upon the amplitude of the shear distortion,  $t$ , is shown in the inset of Fig. 2. We see that  $u_{\min}$  remains equal to zero up to a critical value of  $t = t^*$  which depends on pressure, and that it saturates to  $1/4$  for  $t = 1$ . This behavior is typical of the order parameter at a second-order phase transition, and it indicates therefore that a phonon frequency

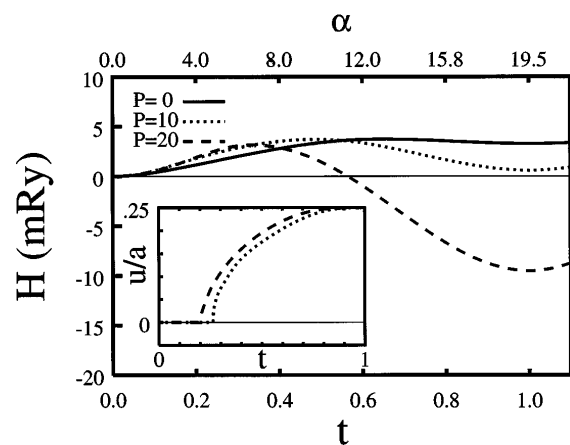


FIG. 2. Enthalpy vs angle of deformation for different values of the applied external pressure. In the inset we show the corresponding values of the amplitude of the lattice distortion,  $u$ .

softens when the shear distortion becomes larger than  $t^*$ . This fact is illustrated in Fig. 3 whose upper panel displays the frequency of the  $M_2^-$  phonon mode as a function of the shear distortion,  $t$ , for different values of the applied pressure. As one sees, at any non-negative pressure, the  $M_2^-$  frequency vanishes for some critical value of  $t$ ,  $t^*$ , which becomes smaller the larger is the applied pressure. We conclude that a second-order phase transition whose order parameter is the amplitude of the  $M_2^-$  distortion,  $u$ , would occur upon application of a shear deformation, when its amplitude  $t$  reaches the critical value  $t^*$ . The lower panel of Fig. 3 shows the dependence of the energy gap,  $E_g$ , upon  $t$ , for different pressures. The filled symbols indicate the data obtained for the values of  $u$  which minimize the crystal energy at the given value of  $t$ ,  $u = u_{\min}(t)$ , whereas the open symbols correspond to  $u = 0$ . One sees that there is a marked correlation between the closing of the gap and the softening of the phonon and that the atomic distortion induced by the phonon softening acts so as to oppose the tendency to metallization.

The mechanisms driving the softening of the  $M_2^-$  phonon are indeed strictly related to the metallization of CsH under an applied pressure and/or shear deformation. At equilibrium ( $P = 0$ ,  $t = 0$ ), the maximum of the valence band is practically degenerate between the  $R \equiv (\frac{1}{2}\frac{1}{2}\frac{1}{2})$  and  $X \equiv (00\frac{1}{2})$  points of the BZ, and the minimum of the conduction bands lies at the  $R$  point. A

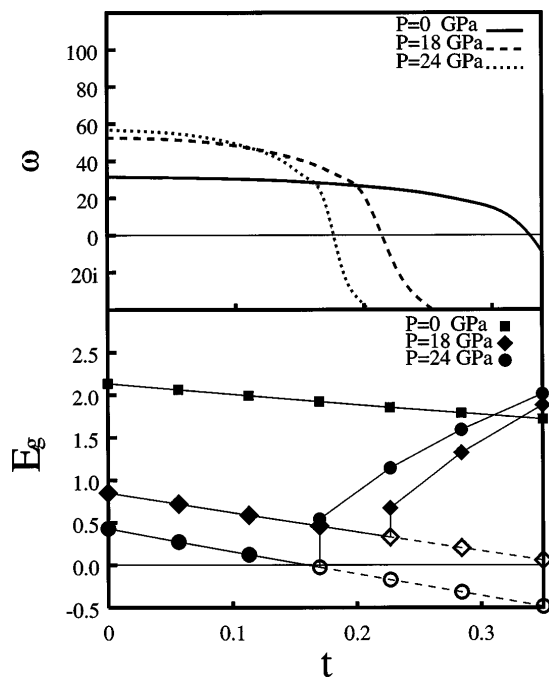


FIG. 3. Upper panel: frequency of the  $M_2^-$  phonon mode ( $\text{cm}^{-1}$ ) as a function of the amplitude of the shear deformation,  $t$ , for different pressures. Lower panel: fundamental energy gap (eV) as a function  $t$  for different pressures. Full symbols indicate data corresponding to the value of the atomic-distortion parameter,  $u$ , which minimizes the crystal energy for the given value of  $t$ ,  $u = u_{\min}(t)$ , whereas the open symbols correspond to  $u = 0$ . The lines are guidelines for the eye.

small applied pressure lifts the degeneracy between the valence-band maxima, raising the  $X$  point with respect to  $R$ . The resulting fundamental band gap,  $E_g$ , corresponds therefore to a  $X \rightarrow R$  transition, whose transferred momentum is  $M \equiv (\frac{1}{2}\frac{1}{2}0)$ , i.e., the wave vector of the phonon which goes soft. In Fig. 4 we display the electronic energy bands of CsH at  $P = 17.5$  GPa, for ( $t = 0, u = 0$ ), for ( $t = 0.3, u = 0$ ), and for ( $t = 0.3, u = 0.086$ ), where the latter value of  $u$  corresponds to  $u_{\min}(t = 0.3)$ , i.e., the value which minimizes the crystal energy for the given value of  $t$ . In the distorted structure—corresponding to a nonvanishing value of  $t$ —the  $R$  and  $X$  points are folded to the same point of the BZ, and so are the  $\Gamma$  and  $M$  points. The gap, which is indirect in cubic symmetry, becomes thus direct in the distorted structure. We see that the shear distortion considerably favors metallization, and thus enhances the screening of the phonon frequencies at the  $M$  point of the cubic BZ. The atomic distortion corresponding to  $u = u_{\min}$  acts so as to reopen the gap. As one sees in Fig. 3, at small pressures, the  $M_2^-$  phonon frequency softens almost for the same values of  $t$  for which the gap closes, whereas for pressure larger than  $\approx 18$  GPa, it takes a larger value of  $t$  to soften the phonon frequency than to close the gap. If the bands were parabolic around the valence- and conduction-band edges, the phonon would go soft at the metallization. In fact, the independent-electron polarizability,  $\chi_0(\mathbf{q}_M)$ , would diverge logarithmically in this case [20], and the restoring force for a lattice distortion of wave vector  $\mathbf{q}_M$  would correspondingly vanish. When the valence and conduction bands have different shapes, the logarithmic divergence would no longer hold, and all that can be said in this case is that the more these shapes are similar, the more metallization contributes to the phonon softening. In any event, when the amplitude of the shear distortion is larger than  $t^*$ , the spontaneous atomic distortion due to phonon softening reopens the band gap and makes the orthorhombic phase insulating, in agreement with the behavior of  $E_g$  found in [21].

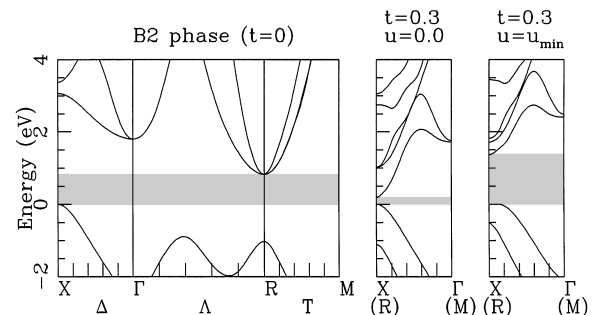


FIG. 4. Electron energy bands of CsH near the fundamental energy gap (which is indicated by the shadowed area) at an applied pressure of 17.5 GPa. Left: cubic  $B2$  structure. Middle: structure corresponding to a finite shear distortion, with no microscopic atomic distortion ( $u = 0$ ). Right: same shear distortion, including a microscopic distortion which minimizes the crystal energy for the given value of  $t$ ,  $u = u_{\min}(t)$ .

The softening of the  $M_2^-$  frequency in correspondence to some value of the shear distortion could have been expected on the basis of symmetry considerations. To see this, let us consider the crystal energy as a function of  $t$  and  $u$ ,  $E(t, u)$ . Crystal symmetry requires that  $E(t, u) = E(\pm t, u) = E(t, -u) = E(t + 2, u \pm \frac{1}{2})$ . These relations imply that  $E(t, u)$  is stationary at the point  $(t, u) = (2, 0)$ . This point lies in between the four equivalent minima at  $(0, 0)$ ,  $(2, \pm \frac{1}{2})$ , and  $(4, 0)$ . Assuming that the energy landscape is simple, we arrive at the conclusion that  $(2, 0)$  is a maximum. In particular, one has that  $\partial^2 E / \partial u^2 < 0$ , and hence there exists a value of  $0 < t < 2$  for which  $\omega_{M_2^-}^2 \sim \partial^2 E / \partial u^2 = 0$ . Further analysis of the energy landscape shows that the presence of the  $M_2^-$  phonon softening upon a small shear deformation (with  $t^* < 1$ ) is a necessary condition for the existence of the observed first-order transition to the orthorhombic structure. The orthorhombic phase corresponds to the  $(1, \frac{1}{4})$  point in the  $(t, u)$  plane which is also stationary because of symmetry. This point is located halfway between the two points  $(1, 0)$  and  $(1, \frac{1}{2})$  which are equivalent by symmetry and stationary with respect to variations of  $u$  ( $\partial E / \partial u = 0$ ). If  $t^*$  were larger than 1,  $\partial^2 E / \partial u^2$  would be positive at  $(1, 0)$  and  $(1, \frac{1}{2})$ , and therefore the assumption of a simple energy landscape would imply that  $(1, \frac{1}{4})$  is a maximum with respect to  $u$ , and the orthorhombic structure unstable. It is easy to see that a first-order transition with a discontinuous variation of  $u$  would occur in this case as the shear distortion crosses  $t = 1$ . In fact, in this case the line  $(t, 0)$  is stable with respect to variations of  $u$ , up to  $t = 1$ . For  $t > 1$  one has that  $E(t, \frac{1}{2}) < E(t, 0)$ . Hence, a discontinuous jump in  $u$  would occur at  $t = 1$  where  $E(t, \frac{1}{2}) = E(t, 0)$ . Arguments similar to those expounded above show that for  $t^* < 1$  the  $(1, \frac{1}{4})$  point is a minimum in the  $u$  direction, while nothing can be concluded in principle for other directions, but the fact that local stability is allowed. Our calculations indicate that in the present case  $t^* < 1$  and that the CrB structure is indeed locally stable. For pressures higher than 11 GPa (15 GPa within GC), this structure is favored with respect to the cubic one, thus giving rise to a first-order transition.

In conclusion, we have shown that the cubic-to-orthorhombic phase transformation recently observed to occur in CsH at an applied pressure of  $\sim 17$  GPa is first order and results from the combination of a shear deformation and an atomic distortion associated with an  $M_2^-$  phonon mode. The latter instability is caused by an enhancement of the electronic screening due to the incipient metallization of this material, and would give rise to a *second-order* transformation if the material were subject to a shear stress, rather than to a hydrostatic pressure.

We would like to thank J.-M. Besson and E. Tosatti for very useful discussions.

\*Electronic addresses: saitta@sissa.it, alfe@sissa.it, degironc@sissa.it, baroni@sissa.it or baroni@cecam.fr

- [1] H.K. Mao, *Simple Molecular Systems at Very High Density*, edited by A. Polian, P. Loubeyre, and N. Boccaro, NATO ASI, Ser. B Vol. 186 (Plenum, New York, 1989), p. 221.
- [2] E. Madelung, Phys. Z. **19**, 524 (1918); P. O. Ewald, Ann. Phys. (Leipzig) **64**, 253 (1921).
- [3] T.-L. Huang and A. Ruoff, Phys. Rev. B **29**, 1112 (1984); T.-L. Huang, K. E. Brister, and A. L. Ruoff, Phys. Rev. B **30**, 2968 (1984); Y. K. Vohra, K. E. Brister, S. T. Weir, S. J. Duclos, and A. L. Ruoff, Science **231**, 1136 (1986).
- [4] E. Knittle and R. Jeanloz, Science **223**, 53 (1984); J. Phys. Chem. Solids **46**, 1179 (1985); E. Knittle, A. Rudy, and R. Jeanloz, Phys. Rev. B **31**, 588 (1985).
- [5] K. Asaumi, Phys. Rev. B **29**, 1118 (1984).
- [6] Y. K. Vohra, S. J. Duclos, and A. L. Ruoff, Phys. Rev. Lett. **54**, 570 (1985).
- [7] N. E. Christensen and S. Satpathy, Phys. Rev. Lett. **55**, 600 (1985); S. Satpathy, N. E. Christensen, and O. Jepsen, Phys. Rev. B **32**, 6793 (1985).
- [8] S. Baroni and P. Giannozzi, Phys. Rev. B **35**, 765 (1987).
- [9] M. Buongiorno Nardelli, S. Baroni, and P. Giannozzi, Phys. Rev. Lett. **69**, 1069 (1992); Phys. Rev. B **51**, 8060 (1995).
- [10] S. J. Duclos, Y. K. Vohra, A. L. Ruoff, S. Filipek, and B. Baranowski, Phys. Rev. B **36**, 7664 (1987).
- [11] H. D. Hochheimer, K. Strossner, W. Honle, B. Baranowski, and S. Filipek, Z. Phys. Chem. **143**, 139 (1985).
- [12] I. O. Bashkin, V. F. Degtyareva, Y. M. Dergachev, and E. G. Ponyatovskii, Phys. Status Solidi (B) **114**, 731 (1982).
- [13] K. Ghandehari, H. Huo, A. L. Ruoff, S. S. Trail, and F. J. Di Salvo, Phys. Rev. Lett. **74**, 2264 (1995).
- [14] P. Hohenberg and W. Kohn, Phys. Rev. **136**, B864 (1964); W. Kohn and J. L. Sham, Phys. Rev. **140**, A1133 (1965).
- [15] In spite of the variety of available GC-DFT we stick to a *standard* representative choice: exchange from A. D. Becke, Phys. Rev. A **38**, 3098 (1988) and correlation from J. P. Perdew, Phys. Rev. B **33**, 8822 (1986).
- [16] D. R. Hamann, M. Schlüter, and C. Chiang, Phys. Rev. Lett. **43**, 1494 (1979); L. Kleinman and D. M. Bylander, Phys. Rev. Lett. **48**, 1425 (1982).
- [17] S. Baroni, P. Giannozzi, and A. Testa, Phys. Rev. Lett. **58**, 1861 (1987); P. Giannozzi, S. de Gironcoli, P. Pavone, and S. Baroni, Phys. Rev. B **43**, 7231 (1991).
- [18] N. Moll, M. Bockstedte, and M. Scheffler, Phys. Rev. B **52**, 2550 (1995).
- [19] The analysis which follows is based on LDA calculations. Our conclusions, of course, do not depend on the form of the exchange-correlation functionals.
- [20] The mathematical mechanism determining the logarithmic divergence of  $\chi_0$  is essentially the same as that responsible for the excitonic instability of semimetals, as explained, e.g., in W. Kohn, in *Many Body Physics*, edited by C. DeWitt and R. Balian, Proceedings of the Les Houches Summer School (Gordon and Breach, New York, 1968), p. 353.
- [21] K. Ghandehari, H. Huo, A. L. Ruoff, S. S. Trail, and F. J. Di Salvo, Solid State Commun. **95**, 385 (1995).